



# The effect of surface stress on the configurational equilibrium of voids and cracks

Chien H. Wu\*

*Department of Civil and Materials Engineering, University of Illinois at Chicago, 842 West Taylor Street, Chicago, IL 60607-7023, USA*

Received 31 July 1998; received in revised form 1 March 1999

---

## Abstract

The title problem is studied for a linear surface energy density with two surface stress coefficients. In terms of a Young's modulus  $E$  and an applied traction  $T$ , the perturbation of a smooth (equilibrium or nonequilibrium) configuration affected by a surface stress  $\Sigma_0$  is proportional to  $\Sigma_0 T/E$ , which is small but depends on the sign of  $T$ . It is shown that, through the existence of an interaction energy between the applied traction and the surface stress, a Griffith crack can actually be strengthened (weakened) by a crack-parallel tension (compression) via surface stress, an intuitively reasonable conclusion that does not follow from linear elasticity. In general, surface stress can effectively reduce an *applied stress-intensity factor* to a lower *effective stress-intensity factor*. © 1999 Elsevier Science Ltd. All rights reserved.

*Keywords:* Surface stress; Configuration (energy) equilibrium; Toughness enhancement

---

## 1. Introduction

When an elastic body, characterized by a Young's modulus  $E$  and a linear dimension  $a_0$ , is subjected to a traction of magnitude  $T$ , the volume elastic energy  $U_e$  is of the order of magnitude given by

---

\* Tel.: +1-312-413-2644; fax: +1-312-996-2426.

*E-mail address:* cwu@uic.edu (C.H. Wu)

$$U_e = O(a_0^3 T^2 / E). \quad (1)$$

At the same time, if a constant surface energy density  $\Gamma_0$  is sufficient to describe the surface response, the total surface free energy  $U_s$  is

$$U_s = O(a_0^2 \Gamma_0). \quad (2)$$

The so-called surface effect becomes significant if

$$U_s / U_e \approx O(1). \quad (3)$$

For example, when aluminum ( $E = 7 \times 10^{10}$  N/m<sup>2</sup>,  $\Gamma_0 = 1$  J/m<sup>2</sup>) is subjected to a high level of stress, say,  $T = 4 \times 10^8$  N/m<sup>2</sup>, the above consideration yields

$$a_0 = O(10^{-6} \text{ m}), \quad (4)$$

with an accompanying strain

$$T/E = O(10^{-2}). \quad (5)$$

Once the condition (3) is met, the relative importance of the volumetric and surface portions of the total energy may be altered by a change in the shape of the surface. Thus, the configurational equilibrium of a solid or, more specifically, a solid-surface system may be altered by surface diffusion. The morphological instability of surfaces of stressed solids is such a problem that has received the most attention (Asaro and Tiller, 1972; Grinfeld, 1986; Srolovitz, 1989; Gao, 1991; Freund, 1995; Spencer and Meiron, 1994; Yang and Srolovitz, 1994). There is also the class of problems dealing with diffusive cavity growth and the subsequent formation of cracks (Rice and Chuang, 1981; Gao, 1995; Chiu and Gao, 1993; Suo and Wang, 1994; Wang and Suo, 1997).

What is fundamental to the aforementioned results is a chemical potential  $\Psi$  defined by

$$\Psi = (W - \Gamma_0 K) \Omega \quad (6)$$

where  $W$  is the strain energy density,  $\Gamma_0$  an assumed constant surface energy density,  $K$  the mean curvature of the surface, and  $\Omega$  the atomic volume, all expressed in terms of a chosen referential configuration. This form of chemical potential is known to be incomplete (Murr, 1975; Leo and Sekerka, 1989), and a full nonlinear expression, together with its dual representation in spatial form, may be found in Wu (1996). The same result, together with additional orientation dependence, may also be derived from a rate calculation (Freund, 1997). An even more comprehensive treatise may be found in the most recent work of Norris (1998). It suffices to say that if the surface energy density is assumed to be a constant at the outset, the resulting chemical potential will turn out to be incomplete.

In a plane strain setting, the deformation of a surface is defined by a single surface stretch ratio  $\Lambda$ . The surface energy density  $\Gamma$  is, in general, a function of

$\Lambda$ , i.e.  $\Gamma = \Gamma(\Lambda)$ . The immediate consequence is a surface stress  $\Sigma$  defined by

$$\Sigma = \partial\Gamma/\partial\Lambda, \quad (7)$$

which is not found in the incomplete expression (6). In this paper,  $\Gamma$  is assumed to be linear in  $\Lambda$ , viz.

$$\Gamma = \sigma_o + \Sigma_o\Gamma = (\sigma_o + \Sigma_o) + \Sigma_o(\Lambda - 1) \quad (8)$$

where  $\sigma_o$  and  $\Sigma_o$  are two surface stress coefficients. It follows from the definition of  $\Gamma$  that the energy required in forming a new unit area of surface is  $\Gamma_o = \sigma_o + \Sigma_o$ . Also, the surface stress is a constant residual stress  $\Sigma_o$ . The main objective of this paper is to determine the effect of  $\Sigma_o$  on some of the known results obtained on the basis of the incomplete chemical potential.

The energy (8) may be extended to include a quadratic term in  $(\Lambda-1)$ , so that the surface stress also depends linearly on  $\Lambda-1$ . This is the theory investigated by Gurtin and Murdoch (1978), where a number of solutions to what was termed a ‘mechanical theory’ were obtained. Mechanical theories deal with the deformational aspect of solids. Our emphasis here is more on an ‘energy theory’ dealing with configurational changes.

In the presence of a surface curvature  $1/r$ , the effect of  $\Sigma_o$  on the solid boundary is a normal traction  $\Sigma_o/r$ . If  $r$  is of the order of  $a_o$  of (1), then the volume elastic energy  $U_e$  derived from an applied traction  $T$  and an additional surface stress-induced traction  $\Sigma_o/a_o$  may be found to consist of three terms:

$$U_e: a_o^3 T^2/E, \quad a_o^2 T \Sigma_o/E, \quad a_o \Sigma_o^2/E \quad (9)$$

where the middle term may be identified with an interaction energy, the result of coupling of two loading systems. It is commonly accepted that  $\Sigma_o$  and  $\Gamma_o$  are of the same order of magnitude. Then

$$(a_o^2 T \Sigma_o/E)/U_s = O(T/E), \quad (10)$$

which implies that the interaction energy is a second order effect. It also indicates that the third term of (9) is even less significant. The inclusion of the interaction energy, however, is important in that it breaks the *stress symmetry* so that the sign of  $T$  actually has a role in the final result (Grilhe, 1993; Wu, Hsu and Chen, 1998).

When the interaction energy is included in the consideration of a Griffith crack of length  $2a_o$ , we have found that the effect of a crack-parallel tension is an increase in the critical value for the applied stress-intensity factor. This result, while second order and intuitively obvious, appears to be new in that it cannot be proved in the context of linear elasticity.

Surface stress enters a problem through its interaction with a nonzero surface curvature. The surface stress  $\Sigma = \Sigma_o$  actually couples with the curvature of the deformed surface which, in terms of linear elasticity, may be approximated by the curvature in the reference configuration. This was implicitly assumed in obtaining

(9). If a crack is deformed by a nonzero stress-intensity factor, the curvature in the neighborhood of a tip is large. This large curvature, interacting with the surface stress  $\Sigma_o$ , is capable of reducing an *applied stress-intensity factor* to a lower *effective stress-intensity factor*. This reduction is carried out by an approximate calculation, and is found to be of first order in that it depends only on  $\Sigma_o/\Gamma_o$ . Chuang (1987) had similar considerations and results.

## 2. Elasticity with surface energy

### 2.1. Kinematics

We consider plane strain deformations of a body whose plane section is identified with a doubly-connected two-dimensional region  $B$  in its reference configuration, Fig. 1. The deformation of the body is described by mappings from  $B$  to two-dimensional region  $b$ . A material particle is labeled by its position vector  $\mathbf{Z} = Z_1 \mathbf{e}_1$  in  $B$ , and its position in  $b$  is denoted by  $\mathbf{z} = z_i \mathbf{e}_i$ , in which  $\{\mathbf{e}_1, \mathbf{e}_2\}$  is a set of fixed unit vectors in the plane under consideration, and  $z_i$  and  $Z_1$  are the Cartesian coordinates of a particle in  $b$  and  $B$ , respectively. The deformation is then defined by a displacement  $\mathbf{u}$ , so that

$$\mathbf{z} = \mathbf{Z} + \mathbf{u}(\mathbf{Z}), \quad \mathbf{Z} \in B. \quad (11)$$

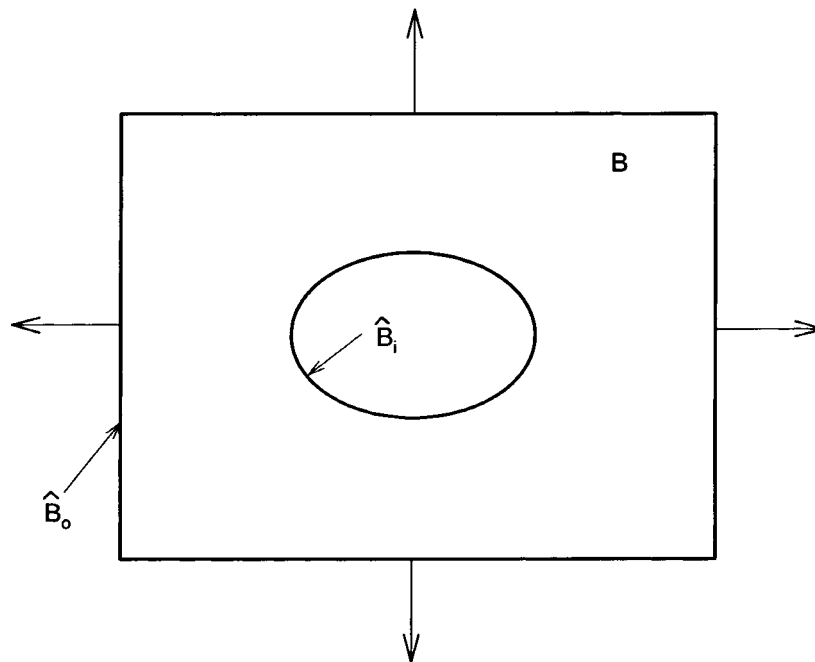


Fig. 1. The cross section of an arbitrary cylindrical void.

The deformation gradient tensor  $\mathbf{F}$  is defined by

$$\mathbf{F} = \mathbf{Grad} \mathbf{z} = \mathbf{I} + \mathbf{Grad} \mathbf{u}, \quad (12)$$

where  $\mathbf{Grad}$  is the gradient operator in  $B$  and  $\mathbf{I}$  the identity.

Let the boundary  $\hat{B}$  of  $B$  be parametrized by its arclength  $L$ , i.e.

$$\hat{B}:\mathbf{Z} = \mathbf{X}(L) = X_1(L)\mathbf{e}_1 \quad (13)$$

where the positive sense of  $L$  is chosen in such a way that on moving in the positive sense along  $\hat{B}$ ,  $B$  lies to the left. The positive exterior normal  $\mathbf{N}$  is simply given by

$$\mathbf{N} = \mathbf{X}'(L) \times \mathbf{e}_3 \quad (14)$$

where  $\mathbf{e}_3 = \mathbf{e}_1 \times \mathbf{e}_2$  and  $\mathbf{X}'(L)$  is the tangent to the boundary. We have

$$\mathbf{X}'' = \mathbf{N}/R \quad (15)$$

where  $1/R$  is the curvature of  $\hat{B}$ . The image of  $\hat{B}$  in  $b$  is the boundary  $\hat{b}$  defined by

$$\hat{b}:\mathbf{z} = \mathbf{z}(l) \quad (16)$$

where  $l$  is the arc length along  $\hat{b}$ . It follows from (11), (12) and the above that

$$\mathbf{x}(l) = \mathbf{X}(L) + \mathbf{u}(\mathbf{X}(L)), \quad (17)$$

$$\mathbf{x}' = \mathbf{F}\mathbf{X}' \, dL/dl, \quad (18)$$

where  $\mathbf{x}'(l)$  is just the tangent to the deformed boundary. The stretch  $\Lambda$  of  $\hat{B}$  is

$$\Lambda^2 = (dl/dL)^2 = \mathbf{F}\mathbf{X}' \cdot \mathbf{F}\mathbf{X}'. \quad (19)$$

The outward normal  $\mathbf{n}$  to  $\hat{b}$  is

$$\mathbf{n} = \mathbf{x}'(l) \times \mathbf{e}_3, \quad (20)$$

and

$$\mathbf{x}'' = \mathbf{n}/\rho \quad (21)$$

where  $1/\rho$  is the curvature of  $\hat{b}$ .

The boundary  $\hat{B}$  of the doubly connected region  $B$  consists of an interior boundary  $\hat{B}_i$  and an exterior boundary  $\hat{B}_o$ . It is assumed that standard traction conditions of elasticity are prescribed on  $\hat{B}_o$ . The interior boundary, though, is further endowed with a surface energy of surface deformation.

## 2.2. Bulk and surface energies

Let  $W(\mathbf{F})$  and  $\Gamma(\Lambda)$  denote, respectively, the bulk and surface energy densities

per unit reference volume and surface area. We write the potential energy  $\Pi$  for the system as follows:

$$\Pi = U_e + U_s - V \quad (22)$$

where

$$U_e = \int_B W \, dA, \quad U_s = \int_{\hat{B}_i} \Gamma \, dL, \quad (23)$$

and  $V$  is the work done by the traction applied on  $\hat{B}_o$ . For a virtual displacement,  $\delta \mathbf{u}$ , we have

$$\delta V = \int_{\hat{B}_o} \mathbf{P}^{(o)} \cdot \delta \mathbf{u} \, dL = \int_{\hat{b}_o} \mathbf{T}^{(o)} \cdot \delta \mathbf{u} \, dl \quad (24)$$

where  $\mathbf{P}^{(o)}$  and  $\mathbf{T}^{(o)}$  ( $\mathbf{P}^{(o)} = \Lambda \mathbf{T}^{(o)}$ ) are applied boundary traction. The result of taking variation of  $\Pi$  and then converting the outcome in terms of the spatial configuration is (Wu, 1996):

$$\delta \Pi = - \int_b T_{ij,i} \delta u_j \, da + \int_{\hat{b}_i} \left[ T_{ij} n_i - \frac{d}{dl} (\Sigma x'_j) \right] \delta u_j \, dl + \int_{\hat{b}_o} (T_{ij} n_i - T_j^{(o)}) \delta u_j \, dl \quad (25)$$

where  $T_{ij}$  is the Cauchy stress tensor and  $\Sigma$  the surface stress given by

$$\Sigma = \partial \Gamma / \partial \Lambda. \quad (26)$$

### 2.3. Surface accretion and chemical potential

Let the interior boundary  $\hat{B}_i$  be given a virtual shape change  $\delta \mathbf{X}$  defined by

$$\delta \mathbf{X} = \mathbf{N} \delta H \quad (27)$$

where  $\mathbf{N}$  is the normal given by (14). The associated potential energy change, denoted by  $\delta^* \Pi$ , was found to be

$$\delta^* \Pi = - \int_B E_{IJ,I} N_J \delta H \, dA + \int_{\hat{B}_i} \left[ E_{IJ} N_I N_J - \frac{d}{dL} (\sigma X'_I) N_I \right] \delta H \, dL \quad (28)$$

where  $E_{IJ}$  is the Eshelby Energy–Momentum tensor given by

$$E_{IJ} = W \delta_{IJ} - (\partial W / \partial F_{IJ}) F_{IJ} \quad (29)$$

and  $\sigma$  a surface quantity defined by

$$\sigma = \Gamma - (\partial\Gamma/\partial\Lambda)\Lambda. \quad (30)$$

We have summarized our earlier results (Wu, 1996) in the form of (25) and (28) because deformational equilibrium is more readily visible in the spatial coordinate, while configurational modulations are easier to see in the reference space. The main objective of this paper is to examine the effect of the boundary condition on  $\hat{b}_i$ , (25), on the line integral of (28). The integrand of this line integral may be made to conform to a chemical potential, but we have found it unnecessary to make such identification for the purpose of this paper.

#### 2.4. Elasticity and linear surface energy

The bulk material is assumed to be linearly elastic, so that the Cauchy stress  $T_{ij}$  of (25) are given by

$$T_{ij} = 2\mu\varepsilon_{ij} + \frac{2\mu\nu}{1-2\nu}\delta_{ij}\varepsilon_{kk}, \quad (31)$$

$$\varepsilon_{ij} = (u_{i,j} + u_{j,i})/2, \quad (i,j,k = 1,2), \quad (32)$$

where  $\mu$  and  $\nu$  are, respectively, shear modulus and Poisson's ratio. For the surface energy, we use the Laplace–Herring model of Grinfeld (1994), which is a linear function of the surface stretch ratio, viz.

$$\Gamma(\Lambda) = \sigma_o + \Sigma_o\Lambda = \Gamma_o + \Sigma_o\varepsilon \quad (33)$$

where  $\sigma_o$  and  $\Sigma_o$  are two surface stress coefficients,  $\varepsilon = \Lambda - 1$ , and

$$\Gamma_o \equiv \Gamma(1) = \sigma_o + \Sigma_o. \quad (34)$$

It follows from the above, (26) and (30) that

$$\Sigma = \partial\Gamma/\partial\Lambda = \Sigma_o, \quad \sigma = \sigma_o. \quad (35)$$

We are not aware of any known theoretical or experimental results dealing with the dependence of  $\Gamma$  on  $\varepsilon$ . However, it is commonly accepted that  $\Gamma$  and  $\Sigma$  are of comparable orders of magnitude (Murr, 1975). Using a plausible argument based on certain universal features derived from experimentally verified binding-energy-distance curves (Rose et al., 1981, 1983; Ferrante et al., 1983), the following result was established by Wu, Hsu and Chen (1998):

$$\Sigma_o = (1 - \nu)\Gamma_o. \quad (36)$$

In any case, the use of (34) and (35) will be adopted in our calculation.

The boundary condition on  $\hat{b}_i$ , the second integral of (25), now becomes

$$T_{ij}n_in_j = \Sigma_o/\rho, \quad T_{ij}n_ix'_j = 0, \quad (37)$$

where we recall, with emphasis, that  $1/\rho$  is the curvature of the deformed surface.

Since the bulk material is assumed to be linearly elastic,  $1/\rho$  is essentially  $1/R$ , the curvature of the undeformed surface, for most cases. One outstanding exception occurs at the tip of a crack, where the flat crack surfaces are opened up into a sharp elliptic nose and the effect of  $\Sigma_o/\rho$ , (37), becomes most pronounced. This last phenomenon will be estimated by an approximate calculation in Section 4.

### 3. A cylindrical void in a solid

#### 3.1. Potential energy

Fig. 1 illustrates the cross section of a cylindrical void in a solid, a two-dimensional specimen subjected to traction applied on the external boundary  $B_o$ , but not on the void surface  $B_i$ . The cross-sectional shape of the void is arbitrary, but not crack like so that the deformed shape,  $b_i$ , may be taken to be the same as the undeformed shape in the context of linear elasticity. Thus, the associated elastic field  $(u_i, \varepsilon_{ij}, T_{ij})$  is solved from

$$T_{ij,i} = 0 \quad \text{in } B, \quad (38)$$

$$T_{ij}n_i = T_j^{(o)} \quad \text{on } \hat{B}_o, \quad (39)$$

$$T_{ij}n_j = \Sigma_o/R \quad \text{on } \hat{B}_i, \quad (40)$$

$$T_{ij}n_i x'_j = 0 \quad \text{on } \hat{B}_i, \quad (41)$$

where we have replaced  $\rho$  in the exact expression, (37), with  $R$ . It is also clear in this setting that  $\mathbf{n}$  is approximately the same as  $\mathbf{N}$ . We find it convenient to split the elastic field into two separate fields, i.e.

$$(u_i, \varepsilon_{ij}, T_{ij}) = (u_i^{(o)}, \varepsilon_{ij}^{(o)}, T_{ij}^{(o)}) + (u_i^{(i)}, \varepsilon_{ij}^{(i)}, T_{ij}^{(i)}) \quad (42)$$

where

$$T_{ij}^{(o)}n_i = T_j^{(o)} \quad \text{on } \hat{B}_o \quad \text{and} \quad T_{ij}^{(o)}n_i = 0 \quad \text{on } \hat{B}_i, \quad (43)$$

$$T_{ij}^{(i)}n_j = \Sigma_o/R \quad \text{and} \quad T_{ij}^{(i)}n_i x'_j = 0 \quad \text{on } \hat{B}_i, \quad (44)$$

$$T_{ij}^{(i)}n_i = 0 \quad \text{on } \hat{B}_o. \quad (45)$$

The strain-energy density  $W$  of (23) is now considered a function of  $\varepsilon_{ij}$ . The elastic energies associated with the three fields of (42) may be separately computed. They are

$$U_e \equiv \int_B W(\varepsilon_{ij}) dA = \frac{1}{2} \int_{\hat{B}_o} \mathbf{T}^{(o)} \cdot \mathbf{u} dL + \frac{1}{2} \int_{\hat{B}_i} \frac{\Sigma_o}{R} \mathbf{n} \cdot \mathbf{u} dL, \quad (46)$$

$$U_e^{(o)} \equiv \int_B W(\varepsilon_{ij}^{(o)}) dA = \frac{1}{2} \int_{\hat{B}_o} \mathbf{T}^{(o)} \cdot \mathbf{u}^{(o)} dL, \quad (47)$$

$$U_e^{(i)} \equiv \int_B W(\varepsilon_{ij}^{(i)}) dA = \frac{1}{2} \int_{\hat{B}_i} \frac{\Sigma_o}{R} \mathbf{n} \cdot \mathbf{u}^{(i)} dL. \quad (48)$$

It follows from substituting (42) into (46) and applying (37) and (48) that

$$U_e = U_e^{(o)} + U_e^{(i)} + \frac{1}{2} \int_{\hat{B}_o} \mathbf{T}^{(o)} \cdot \mathbf{u}^{(i)} dL + \frac{1}{2} \int_{\hat{B}_i} \frac{\Sigma_o}{R} \mathbf{n} \cdot \mathbf{u}^{(o)} dL. \quad (49)$$

The total (void) surface energy is

$$U_s = \int_{\hat{B}_i} (\Gamma_o + \Sigma_o \varepsilon_{tt}) dL, \quad (50)$$

which follows from (33) with  $\varepsilon_{tt}$  being the circumferential strain, i.e.

$$\varepsilon_{tt} = -\frac{\mathbf{u} \cdot \mathbf{n}}{R} + \frac{\partial}{\partial L} (\mathbf{u} \cdot \mathbf{x}'). \quad (51)$$

The total surface energy now becomes

$$U_s = \Gamma_o L - \int_{\hat{B}_i} \frac{\Sigma_o}{R} \mathbf{n} \cdot (\mathbf{u}^{(o)} + \mathbf{u}^{(i)}) dL \quad (52)$$

where  $L$  is the total arc length of the cylindrical void. Substituting (49) and (52) into (22), and applying (47) and (48), we obtain the total potential for the elastic solid and void surface

$$\Pi = -U_e^{(o)} + \Gamma_o L - \int_{\hat{B}_i} \frac{\Sigma_o}{R} \mathbf{n} \cdot \mathbf{u}^{(o)} dL - U_e^{(i)} \quad (53)$$

where use has been made of the reciprocal identity

$$\int_{\hat{B}_i} \frac{\Sigma_o}{R} \mathbf{n} \cdot \mathbf{u}^{(o)} dL = \int_{\hat{B}_o} \mathbf{T}^{(o)} \cdot \mathbf{u}^{(i)} dL. \quad (54)$$

### 3.2. A circular cylindrical void filled with fluid

Consider a circular cylindrical void of radius  $a_o$  in the center of a cylinder of radius  $r_o$ . The void is filled with a fluid under pressure  $p$ , and the boundary condition for the solid at  $r = a_o$  is therefore modified by replacing  $\Sigma_o/a_o$  with  $\Sigma_o/a_o - p$ . The plane-strain elastic field, for  $a_o/r_o \leq 1$ , is

$$u_r = \frac{(1+\nu)T^{(o)}a_o}{E} \left[ \frac{a_o}{r} + (1-2\nu)\frac{r}{a_o} \right] - \frac{(1+\nu)(\Sigma_o - pa_o)}{E} \left[ \frac{a_o}{r} + (1-2\nu)\frac{a_o r}{r_o^2} \right], \quad (55)$$

where  $T^{(o)}$  is the applied traction at  $r_o$ , and the two terms are, respectively,  $u_r^{(o)}$  and  $u_r^{(i)}$ . The four terms of the full potential  $\Pi$ , (53), are

$$-U_e^{(o)} = -\frac{\pi(1+\nu)T^{(o)^2}}{E} [(1-2\nu)r_o^2 + 2(1-\nu)a_o^2], \quad (56)$$

$$\Gamma_o L = 2\pi\Gamma_o a_o, \quad (57)$$

$$-\int \left( \frac{\Sigma_o}{R} - p \right) \mathbf{n} \cdot \mathbf{u}^{(o)} dL = 4\pi(1-\nu^2) \frac{T^{(o)}a_o^2}{E} \left( \frac{\Sigma_o}{a_o} - p \right), \quad (58)$$

$$-U_e^{(i)} = -\frac{\pi(1+\nu)}{E} (\Sigma_o - pa_o)^2. \quad (59)$$

The first term of (56) reflects the size of the specimen, while the second, that of the void. Eq. (57) gives the contribution of the constant surface energy  $\Gamma_o$ . The effect of surface stress  $\Sigma_o$  is brought into the picture by (58) and (59).

The total potential  $\Pi$  is now obtained as a function of the void radius. For configurational equilibrium, the energy equation is  $\partial\Pi/\partial a_o = 0$  or

$$\begin{aligned} & \frac{2(1-\nu^2)}{E} \left[ T^{(o)^2} + 2T^{(o)}p + \frac{p^2}{2(1-\nu)} \right] a_o \\ & = \Gamma_o \left[ 1 + 2(1-\nu^2) \frac{\Sigma_o}{\Gamma_o} \frac{T^{(o)}}{E} + (1+\nu) \frac{\Sigma_o}{\Gamma_o} \frac{p}{E} \right]. \end{aligned} \quad (60)$$

Traditionally and for solid surfaces, the surface energy  $\Gamma$ , (60), is taken to be a constant  $\Gamma_o$ , so that  $\partial\Gamma/\partial\Lambda$  is zero. The associated incomplete energy equation may be deduced from (60) by setting  $\Sigma_o$  equal to zero.

Since  $\Gamma_o$  and  $\Sigma_o$  are of comparable orders of magnitude, it is seen from (60) that the effect of  $\Sigma_o$  is of the small order of  $T^{(o)}/E$  or  $p/E$ . While it is not uncommon for the indicated ratios to reach as large as 5%, the contribution of surface stress can only be considered second order in the context of a linear theory defined by (58) and (60). Nevertheless, the result is significant in that it breaks the *stress symmetry*, so that the equilibrium radius is actually affected by the sign of  $T^{(o)}$ . Similar calculations have shown that thin films grown under tension behave differently from those under compression (Wu, Hsu and Chen, 1998).

Finally, if the fluid pressure  $p$  is absent, then

$$U_e^{(i)} = \pi(1 + \nu)\Sigma_0^2 f/E, \quad (61)$$

where  $f = 1$  for the present case of a circular void. For an arbitrary cylindrical void,  $f$  may be obtained in terms of geometric parameters. Since

$$T^{(0)2} a_0/E\Gamma_0 = O(1), \quad (62)$$

by (60), we find

$$U_e^{(i)}/\Gamma_0 a_0 = O(T^{(0)2}/E)^2. \quad (63)$$

The last term of (53) will henceforth be dropped from consideration.

### 3.3. An elliptical void

Let  $a_0$  be the radius of a reference circular void. The family of ellipses having the same area as the circle,  $\pi a_0^2$ , is given by

$$x_1 = a \cos \phi = a_0((1+m)/(1-m))^{1/2} \cos \phi, \quad (64)$$

$$x_2 = b \sin \phi = a_0((1-m)/(1+m))^{1/2} \sin \phi, \quad (65)$$

where  $m = -1, 0, +1$  correspond, respectively, to a vertical slit of length  $2b$ , a circle of radius  $a_0$ , and a horizontal slit of length  $2a$ . In terms of the complex  $z (= x_1 + ix_2)$ -plane, another complex  $\zeta (= \zeta_1 + i\zeta_2)$ -plane, and the mapping

$$z = M(\zeta) = A(\zeta + m/\zeta), \quad A = a_0/(1-m^2)^{1/2}, \quad (66)$$

the family of ellipses is just  $z = M(e^{i\phi})$ . This void is situated in an infinite solid, which is loaded at infinity by  $T_{11} = T_1$ ,  $T_{22} = T_2$  and  $T_{12} = 0$ . The elasticity solution satisfying this loading condition and the traction-free condition on the void surface is given by  $(u_i^{(0)}, \varepsilon_{ij}^{(0)}, T_{ij}^{(0)})$  of (42) and (43). It may be expressed in terms of a single complex function  $\Omega(\zeta)$ , which is holomorphic outside the unit circle in the  $\zeta$ -plane, viz.,

$$\Omega(\zeta) = \frac{A}{4}(T_1 + T_2)\zeta + \left[ \frac{A}{2}(T_1 - T_2) - \frac{Am}{4}(T_1 + T_2) \right] \frac{1}{\zeta}, \quad (67)$$

$$2\mu(u_1^{(0)} + iu_2^{(0)}) = \kappa\Omega(\zeta) + \Omega(1/\bar{\zeta}) - [M(\zeta) - M(1/\bar{\zeta})]\overline{\Omega'(\zeta)}/\overline{M'(\zeta)}. \quad (68)$$

<sup>1</sup>This solution is now used to calculate the first three terms of the potential  $\Pi$  given by (53). If the surface stress is ignored, the potential  $\Pi$  is merely the first two terms of (53), which has been studied by Suo and Wang (1994). We therefore

<sup>1</sup>  $\kappa = 3 - 4\nu$  for plane strain and  $(3 - \nu)/(1 + \nu)$  for plane stress.

concentrate on the determination of the third term, the coupling of the surface stress and the load.

Using the complex representation of the ellipse  $z = M(e^{i\phi})$ , we obtain

$$\frac{dL}{R} = \frac{(1 - m^2)d\phi}{1 + m^2 - 2m \cos 2\phi}. \quad (69)$$

The displacement of the void surface is

$$u_1^{(o)} + iu_2^{(o)} = \frac{(\kappa + 1)A}{8\mu} \left[ (T_1 + T_2) \left( \zeta - \frac{m}{\zeta} \right) + 2(T_1 - T_2) \frac{1}{\zeta} \right] \quad (70)$$

where  $\zeta$  is  $e^{i\phi}$ . Along the void surface

$$\begin{aligned} -\mathbf{n} \cdot \mathbf{u}^{(o)} &= Re \left\{ - (u_1^{(o)} + iu_2^{(o)}) i \frac{d\bar{z}}{dL} \right\} \\ &= \frac{(\kappa + 1)A}{8\mu} (T_1 + T_2) (1 + m^2 - 2m \cos 2\phi)^{1/2} \\ &\quad + \frac{(\kappa + 1)A}{4\mu} (T_1 - T_2) (\cos 2\phi - m) (1 + m^2 - 2m \cos 2\phi)^{-1/2}. \end{aligned} \quad (71)$$

For the body with an elliptic hole and the body with a circular hole, the potential energy differs by

$$\Delta\Pi = \Pi(m, T_1, T_2) - \Pi(0, T_1, T_2) \quad (72)$$

where  $\Pi$  is calculated from the first three terms of (53). We have, for plane strain,

$$\begin{aligned} \Delta\pi &= -\lambda \left[ \frac{m}{1 - m} - \frac{m}{1 + m} \sigma^2 \right] + [p(m) - 1] + c\varepsilon_o \{ (1 + \sigma) p_1(m) - 1 \} \\ &\quad - 2(1 - \sigma) p_2(m) \} \end{aligned} \quad (73)$$

where

$$\begin{aligned} \Delta\pi &= \frac{\Delta\Pi}{2\pi a_o \Gamma_o}, \quad \lambda = \frac{(1 - \nu^2) a_o T_2^2}{E \Gamma_o}, \quad \sigma = \frac{T_1}{T_2}, \quad c = \frac{\Sigma_o}{\Gamma_o}, \\ \varepsilon_o &= \frac{(1 - \nu^2) T_2}{E}. \end{aligned} \quad (74)$$

The functions  $p(m)$ ,  $p_1(m)$  and  $p_2(m)$  are given by

$$\begin{aligned} p(m) &= (1 - m^2)^{-1/2} q(m), \quad p_1(m) = (1 - m^2)^{1/2} q_1(m), \\ p_2(m) &= (1 - m^2)^{1/2} q_1'(m), \end{aligned} \quad (75)$$

where

$$q(m) = \frac{1}{2\pi} \int_0^{2\pi} (1 + m^2 - 2m \cos 2\phi)^{1/2} d\phi, \tag{76}$$

$$q_1(m) = \frac{1}{2\pi} \int_0^{2\pi} (1 + m^2 - 2m \cos 2\phi)^{-1/2} d\phi. \tag{77}$$

For computational purposes we have found the following expansions sufficiently accurate:

$$q(m) = 1 + \frac{1}{4}m^2 + \frac{1}{64}m^4 + \dots, \tag{78}$$

$$q_1(m) = 1 + \frac{1}{4}m^2 + \frac{9}{64}m^4 + \dots \tag{79}$$

Setting  $c = 0$  in (73), we recover Eq. (25) of Suo and Wang (1994). It is seen that while  $\lambda$  is insensitive to the sign of  $T_2$ ,  $\epsilon_0$  is. For a fixed set of system parameters ( $E, \nu, \Gamma_0, \Sigma_0, a_0$ ) and a fixed stress ratio  $\sigma = T_1/T_2$ , the stability of an elliptic void characterized by  $m$  is to be determined in terms of the control stress  $T_2$ . If the effect of surface stress is to be ignored, i.e.  $c=0$ , the most convenient form of a control parameter is  $\lambda$ . This is why the stability investigations of Suo and Wang (1994) are presented in the  $\lambda$ - $m$  plane. For a nonzero  $c$ , the effect of  $\epsilon_0$  must be included. However,  $\epsilon_0$  also depends on the control stress  $T_2$ . Thus we write

$$\epsilon_0 = \pm \delta^{1/2} \lambda^{1/2}, \quad \delta = (1 - \nu^2) \Gamma_0 / a_0 E \propto (T_2/E)^2 \tag{80}$$

<sup>2</sup>where  $\delta$  is another system parameter, and  $\pm$  refers to the sign of  $T_2$ . Finally, we will restrict ourselves to the case

$$0 \leq \sigma = T_1/T_2 \leq 1, \tag{81}$$

so that both  $T_1$  and  $T_2$  are of the same sign. The potential  $\Delta\pi(m, \lambda, \sigma, c^*)$  is now obtained by substituting (75) and (80) into (73):

$$\begin{aligned} \Delta\pi = & -\lambda[(1 - \sigma^2)m + (1 + \sigma^2)m^2](1 - m^2)^{-1} + (1 \\ & - m^2)^{-1/2}q(m) \pm c^* \lambda^{1/2} \{(1 + \sigma)[(1 - m^2)^{1/2}q_1(m) - 1] - 2(1 - \sigma)(1 \\ & - m^2)^{1/2}q'_1(m)\} \end{aligned} \tag{82}$$

where  $c^* = c\delta^{1/2}$  and, for computational purposes,  $q(m)$  and  $q_1(m)$  are the three-term expansions of (78) and (79). Differentiating (82) with respect to  $m$ , we get

---

<sup>2</sup> Confer (63) for order of magnitude of  $\delta$ .

$$\Delta\pi' = \frac{1}{(1-m^2)^2} \left\{ -[(1+m)^2 - (1-m)^2\sigma^2]\lambda + \frac{3}{2}(1-m^2)^{1/2} \left( m - \frac{1}{8}m^3 - \frac{1}{32}m^5 + \dots \right) \pm c^*\lambda^{1/2}(1-m^2)^{3/2} \left[ \frac{1}{2}(1+\sigma) \left( m + \frac{3}{8}m^3 + \frac{45}{32}m^5 + \dots \right) \right. \right. \\ \left. \left. + \dots + (1-\sigma) \left( 1 + \frac{11}{8}m^2 - \frac{9}{2}m^4 + \dots \right) \right] \right\} \quad (83)$$

where, we recall,  $m$  is the shape parameter and  $\lambda$  the control parameter. The equilibrium curve  $\lambda = \lambda_E(m, \sigma, c^*)$  is obtained from

$$\Delta\pi'(m, \lambda_E, \sigma, c^*) = 0. \quad (84)$$

The function  $\lambda_E(m, \sigma, 0)$  is just

$$\lambda_E(m, \sigma, 0) = \frac{3}{2}(1-m^2)^{1/2} \left( m - \frac{1}{8}m^3 - \frac{1}{32}m^5 + \dots \right) / ((1+m)^2 - (1-m)^2\sigma^2) \quad (85)$$

which approximates extremely well the numerical results presented by Suo and Wang (1994) in their Figs. 2–5. Since  $c^* = c\delta^{1/2}$  is small,  $\lambda_E(m, \sigma, c^*)$  may be

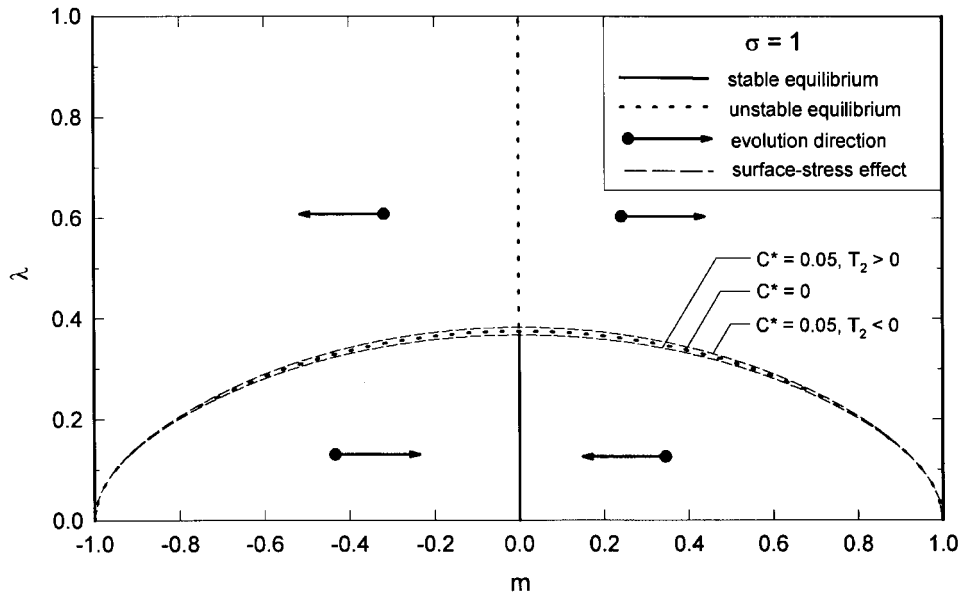


Fig. 2. Equilibrium and stability for  $\sigma = T_1/T_2 = 1$ .

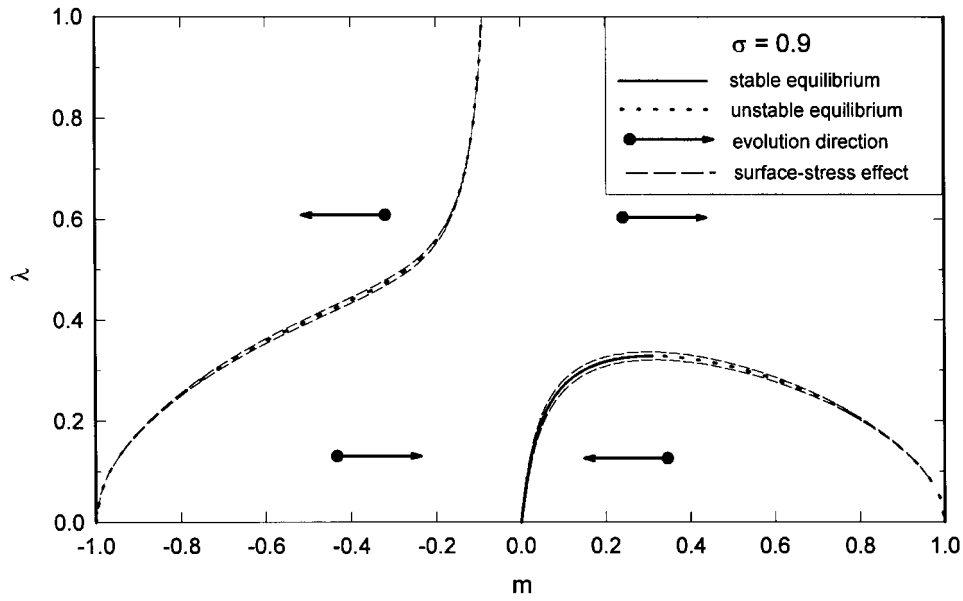


Fig. 3. Equilibrium and stability for  $\sigma = T_1/T_2 = 0.9$ .

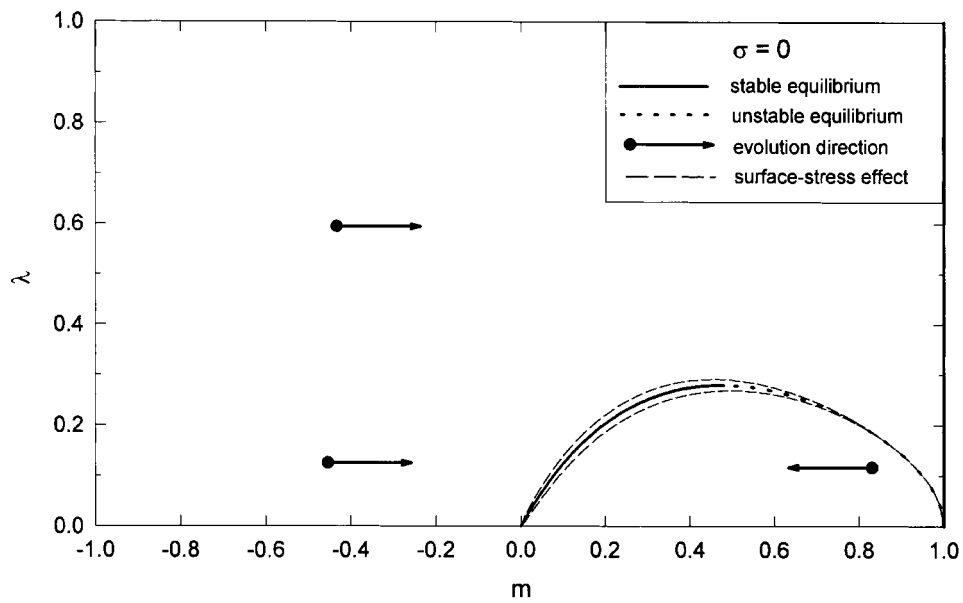


Fig. 4. Equilibrium and stability for uniaxial load  $T_2 \neq 0, T_1 = 0$ .

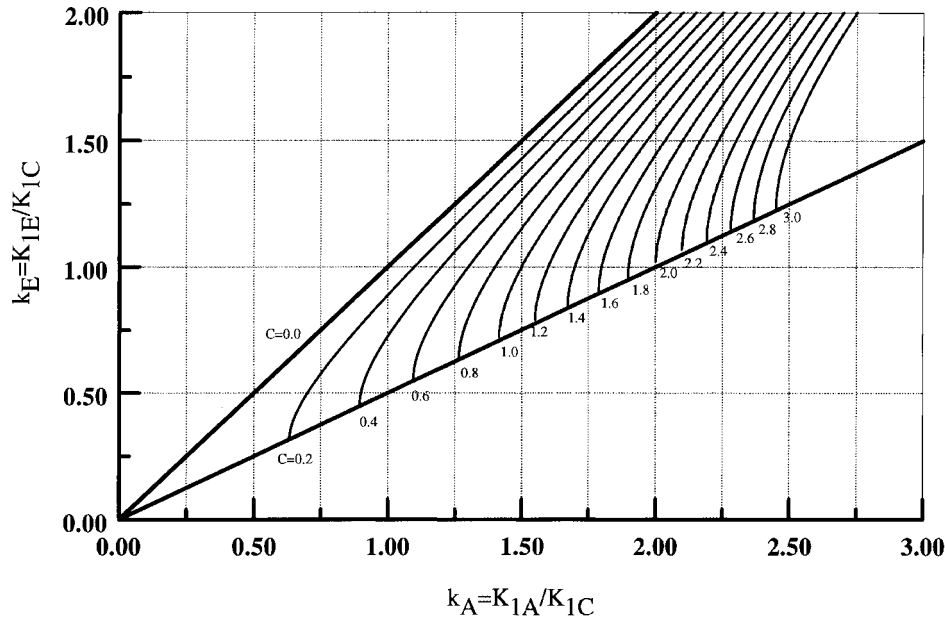


Fig. 5. An applied SIF is reduced to an effective SIF by  $\Sigma_o = C\Gamma_o$ .

approximated by

$$\lambda_E(m, \sigma, c^*) = \lambda_E(m, \sigma, 0) \mp c^* \lambda_E^{1/2}(m, \sigma, 0) g(m, \sigma) \tag{86}$$

where

$$g(m, \sigma) = (1 - m^2)^{3/2} [(1 + m)^2 - (1 - m)^2 \sigma^2]^{-1} \times \left[ \frac{1}{2}(1 + \sigma) \left( m + \frac{3}{8}m^3 + \frac{45}{32}m^5 + \dots \right) + (1 - \sigma) \left( 1 + \frac{11}{8}m^2 - \frac{9}{2}m^4 + \dots \right) \right]. \tag{87}$$

Let  $\lambda = \lambda_c(\sigma, c^*)$  and  $m = m_c(\sigma, c^*)$  be the critical point defined by

$$\lambda_E'(m_c, \sigma, c^*) = 0, \quad \lambda_c = \lambda_E(m_c, \sigma, c^*). \tag{88}$$

We write

$$m_c(\sigma, c^*) = m_c(\sigma, 0) + c^* m_c \tag{89}$$

where  $m_c(\sigma, 0)$  may be directly obtained from (85). A lengthy but straightforward calculation yields, for  $m = m_c(\sigma, 0)$ ,

$$\sigma^2 = (1 + m)^2 \left[ (1 - m^2) \left( 1 - \frac{3}{8}m^2 - \frac{5}{32}m^4 \right) + (m - 2) \left( m - \frac{1}{8}m^3 - \frac{1}{32}m^5 \right) \right] \div (1 - m)^2 \left[ (1 - m^3) \left( 1 - \frac{3}{8}m^2 - \frac{5}{32}m^4 \right) + (m + 2) \left( m - \frac{1}{8}m^3 - \frac{1}{32}m^5 \right) \right]. \tag{90}$$

Substituting (89) into (88) and using (86), we obtain

$$\dot{m}_c = \pm \lambda_E^{1/2}(m_c(\sigma, 0), \sigma, 0) g'(m_c, 0, 0) / \lambda_E''(m_c(\sigma, 0), 0). \tag{91}$$

The formula (90) enables us to obtain  $m_c(\sigma, 0)$  in an inverse manner through direct calculation. Critical values of the control parameter  $\lambda_c(\sigma, c^*)$  are then computed from (86)–(91).

For the case of hydrostatic stress,  $\sigma = T_1/T_2 = 1$  and

$$\lambda_E(m, 1, c^*) = \lambda_E(m, 1, 0) \mp \frac{1}{4} c^* \lambda_E^{1/2}(m, 1, 0) (1 - m^2)^{3/2} \left( 1 + \frac{3}{8}m^2 + \frac{45}{32}m^4 + \dots \right), \tag{92}$$

$$\lambda_E(m, 1, 0) = \frac{3}{8} (1 - m^2)^{1/2} \left( 1 - \frac{1}{8}m^2 - \frac{1}{32}m^4 + \dots \right). \tag{93}$$

The associated critical value  $\lambda_c(1, c^*)$  is

$$\lambda_c(1, c^*) = \lambda_E(0, 1, c^*) = \frac{3}{8} \mp \frac{1}{8} \sqrt{\frac{3}{2}} c^* \tag{94}$$

for  $\pm T_2$ . The implication of (92)–(94) is summarized in Fig. 2. The case for zero surface stress,  $c^* = 0$ , was first discussed by Suo and Wang (1994). It may be shown that for  $\lambda > 3/8$  and  $c^* = 0$ , the potential (82) has a single maximum at  $m = 0$ , and tends to  $-\infty$  as  $m \rightarrow \pm 1$ . When  $\lambda < 3/8$ , the potential has a minimum at  $m = 0$  and two maxima at  $m = \pm m(\lambda)$ , where  $m(\lambda)$  satisfies  $\lambda_E(m(\lambda), 1, 0) = \lambda$ . It also tends to  $-\infty$  as  $m \rightarrow \pm 1$ . Thus, the  $(\lambda, m)$  plane is divided into four regions by  $m = 0$  and  $\lambda = \lambda_E(m, 1, 0)$ . The four possible stable equilibrium configurations are vertical crack ( $m = -1$ ), circle ( $m = 0$ ), and horizontal crack ( $m = 1$ ). For an elliptic void characterized by a shape parameter  $m$  and subjected to the action of a control parameter  $\lambda$ , the direction of its shape evolution follows one of the four heavy arrowheads shown in Fig. 2. It is seen that the effect of a nonzero surface stress is to change the stability boundary slightly.

For  $\sigma = T_1/T_2 = 0.9$ , the implication of (85)–(87) is illustrated in Fig. 3. The  $(\lambda, m)$  plane is still basically divided into four regions, and  $m = \pm 1$  remain to be two possible stable equilibrium configurations. The other stable equilibrium

configuration is a horizontally elongated ellipse. Heavy arrowheads are again used to indicate the shape evolution directions. Finally, the small perturbation in stability boundary due to the presence of surface stress is also given in the figure. The curves plotted in Fig. 3 are typical for all values of  $\sigma$  in the range  $0 < \sigma = T_1/T_2 < 1$ . As  $\sigma \rightarrow 0$ , the curves on the left recede to infinity and disappear altogether when  $\sigma = 0$ . This limiting case is summarized in Fig. 4. It is seen that  $m = -1$  is no longer a possible equilibrium configuration.

Attention is now given to the limiting case of a horizontal slit of vanishing thickness. We find from (77) the property

$$q_1(m) = -\frac{1}{\pi} \ln(1-m) + \dots \quad \text{as } m \rightarrow 1. \quad (95)$$

Substituting the above into (82) and retaining only the singular terms, we get, for tensile  $T_2$ ,

$$\Delta\pi = -\frac{\lambda}{1-m} + [1 - c^*\lambda^{1/2}(1-\sigma)]\frac{2\sqrt{2}}{\pi}(1-m)^{-1/2} + \dots \quad (96)$$

which is associated with a very flat ellipse of axes  $a$  and  $b$  given by (64) and (65). The dimensional form of the above, expressed in terms of  $a$  and other physical variables, becomes

$$\Delta\Pi = -\frac{(1-\nu^2)\pi a^2 T_2^2}{E} + 4\Gamma_o a - \frac{4\Sigma_o(1-\nu^2)T_2 a(1-T_1/T_2)}{E} \quad (97)$$

which is the potential associated with a crack of length  $2a$  when surface-stress effect is also included. The first two terms of (97) are well known, and the last can also be checked by a simple calculation via the third term of (53). For a flat crack, the surface-stress induced solid-surface traction is a pair of point loads, each of magnitude  $2\Sigma_o$ , pointing to each other and acting at  $x_1 = \pm a$ . The displacements of the tips may be straightforwardly calculated from (71). The negative work produced by the forces gives the desired result. The configurational equilibrium condition is obtained by setting to zero the derivative of (97) with respect to  $a$  (not the reference radius  $a_o$ ). This condition, expressed in terms of the applied stress intensity factor

$$K_{1A} = T_2\sqrt{\pi a}, \quad (98)$$

is

$$K_{1A}^2 + 2(1-\sigma)\frac{\Sigma_o}{\sqrt{\pi a}}K_{1A} - \frac{2\Gamma_o E}{(1-\nu^2)} = 0, \quad (99)$$

which reduces to the Griffith condition for  $\Sigma_o = 0$ . For hydrostatic tension ( $\sigma = 1$ ), the critical value of  $K_{1A}$  is not affected by  $\Sigma_o$ . This is so because the displacements of the crack tips are identically zero. For a uniaxial  $T_2$  ( $\sigma = 0$ ) the critical value of

$K_{1A}$  is somewhat reduced by the fact that the  $T_2$ -derived crack tip displacements are co-directional with the  $2\Sigma_0$ -forces.

In general, tensile  $T_1$  enhances the critical value of  $K_{1A}$  while compressive  $T_1$  diminishes it. This is very much in line with the widely held intuition that crack-parallel compression makes it easier to propagate a crack, a proposition that cannot be proved by elasticity. The related deformational stability problem, however, has been shown to agree with the mentioned conception (Wu, 1979, 1980).

Finally, it follows from the identities

$$\frac{\Sigma_0 K_{1A}}{\sqrt{\pi a}} = \Sigma_0 T_2 = \Gamma_0 E \left( \frac{\Sigma_0}{\Gamma_0} \right) \left( \frac{T_2}{E} \right) \quad (100)$$

that the second term of (99) is of the order of  $T_2/E$ , relative to the other two terms. The conclusion of this section is that for regular problems the effect of surface stress is always of the order of (applied stress/ $E$ ). That this is so follows from the strictly linear setup that the radius  $\rho$  of the deformed surface, (37), is replaced by the reference radius  $R$  of (44).

For a flat crack,  $R$  is infinite everywhere except at the tip where  $R$  is actually zero. Upon deformation, however, the crack periphery turns into an ellipse of varying  $\rho$ . This nonlinear effect is estimated via an approximate calculation in the next section.

## 4. Cracks

### 4.1. Kinematics of an ellipse and a stress-intensity-factor generated ellipse

Let us consider an ellipse defined by (64) and (65), i.e.

$$z = x_1 + ix_2 = M(\zeta_0), \quad \zeta_0 = e^{i\phi}. \quad (101)$$

If  $L$  and  $R$  are, respectively, the arclength and radius of curvature along the ellipse, then

$$dL = A[1 + m^2 - 2m \cos 2\phi]^{1/2} d\phi, \quad (102)$$

$$R = A(1 - m^2)^{-1}[1 + m^2 - 2m \cos 2\phi]^{3/2}. \quad (103)$$

At the tips of the major axis,  $x_1 = \pm a = \pm (1 + m)A$ , the radius of curvature is

$$R = R_0 = A(1 - m)^2/(1 + m) = a(1 - m)/(1 + m)^2 = a(b/a)^2. \quad (104)$$

Thus, for an almost flat ellipse defined by  $\beta = 1 - m \ll 1$ , the ellipse nose radius is

$$R_o = \frac{1}{4}a\beta^2. \quad (105)$$

Expressed in terms of  $x_1$ , the curvature may be written

$$\frac{1}{R} = \frac{1}{8}a^2(1-m)(1+m)^2 \left[ \frac{(1+m)^2}{4m}a^2 - x_1^2 \right]^{-3/2} \quad (106)$$

which tends to

$$\frac{1}{R} = \frac{1}{2}a^2\beta \left[ \left( 1 + \frac{1}{4}\beta^2 \right) a^2 - x_1^2 \right]^{-3/2}, \quad (107)$$

for  $\beta \ll 1$ .

Consider now a crack of length  $2a$  ( $|x_1| < a$ ,  $x_2=0$ ). It is opened up by remote stresses  $T_{11}=T_{22}=T$ ,  $T_{12}=0$ , so that, for plane-strain condition,  $u_1(x_1, \pm 0)=0$  and

$$u_2(x_1, \pm 0) = \pm \frac{2a(1-\nu^2)}{E} \frac{K_1}{\sqrt{\pi a}} \left[ 1 - \left( \frac{x_1}{a} \right)^2 \right]^{1/2}. \quad (108)$$

where  $K_1 = T\sqrt{\pi a}$  is the stress intensity factor. The opening of the crack is an ellipse of major axis  $a$  and minor axis  $b$  defined by

$$b = \frac{2a(1-\nu^2)T}{E} = \frac{2a(1-\nu^2)}{E} \frac{K_1}{\sqrt{\pi a}}. \quad (109)$$

It follows from the purely geometric relations (101)–(107) that, for the above stress-intensity-factor generated ellipse,

$$\beta = 1 - m = 2\frac{b}{a} = \frac{4(1-\nu^2)}{E} \frac{K_1}{\sqrt{\pi a}}. \quad (110)$$

Substituting the above into (105), we obtain

$$R_t(K_1) = \frac{4(1-\nu^2)K_1^2}{\pi E^2}, \quad (111)$$

which is the crack-tip radius generated by a stress-intensity factor  $K_1$ .

#### 4.2. The linear elasticity problem of a very flat elliptic void

Let us now consider the well-posed problem defined by (44) and (45). The inner boundary  $B_i$  is just the ellipse (101), and the outer boundary recedes to infinity. It is clear from (44) that the traction and an arc element  $dL$  is a normal tensile force  $(\Sigma_o/R) dL \mathbf{N}$ , where both  $R$  and  $\mathbf{N}$  are continuously varying. We have so far not

been able to solve this linear problem explicitly in general terms, but the most important information we need is the behavior near  $x_1 = \pm a$  for  $\beta = 1 - m \ll 1$ .

The  $x_2$ -component of the aforementioned normal tensile force is

$$\pm \frac{\Sigma_o}{R} N_2 dL \mathbf{e}_2 = \pm \frac{\Sigma_o}{R} dx_1 \mathbf{e}_2 \tag{112}$$

where ‘+’ applies to the lower surface of the ellipse, and ‘-’ the upper surface. For  $\beta = 1 - m \ll 1$ , the ellipse is almost a crack. To estimate the elastic deformation, we simply place the traction calculated from a flat ellipse, (112), on the upper and lower surfaces of a crack. If we denote the solution by  $T_{ij}^{(i)}(x_1, x_2)$  then

$$T_{22}^{(i)}(x_1, \pm 0) = \frac{\Sigma_o}{2} a^2 \beta \left[ \left( 1 + \frac{1}{4} \beta^2 \right) a^2 - x_1^2 \right]^{-3/2} \tag{113}$$

and  $T_{12}^{(i)}(x_1, \pm 0) = 0$  for  $|x_1| \leq a$ . The net effect of the above is a negative stress-intensity factor  $K_{1\Sigma}$  given by

$$\begin{aligned} K_{1\Sigma} &= -\frac{1}{\sqrt{\pi a}} \int_{-a}^a T_{22}^{(i)}(x_1, \pm 0) \sqrt{\frac{a+x_1}{a-x_1}} dx_1 \\ &= -\frac{1}{\sqrt{\pi a}} \int_0^a T_{22}^{(i)}(x_1, \pm 0) \frac{d(x_1^2)}{(a^2 - x_1^2)^{1/2}} \end{aligned} \tag{114}$$

in which use has been made of the fact that  $T_{22}^{(i)}$  is even in  $x_1$ . Integrating and retaining only the leading term in  $\beta$ , we get

$$K_{1\Sigma}(R_o) = -\frac{4\Sigma_o}{\sqrt{\pi a \beta}} = -\frac{2\Sigma_o}{\sqrt{\pi R_o}} \tag{115}$$

where (105) has been used. This result indicates that as the flat ellipse-nose radius  $R_o$  tends to zero, the surface stress induced stress intensity factor tends to minus infinity. Thus, if  $R_o$  is actually produced by a small applied stress-intensity factor, the effect of (105) is to close the smooth ellipse nose into a cusp.

### 4.3. Approximate nonlinear effect

When a crack is opened up by an *applied stress-intensity factor*  $K_{1A}$ , the theory of linear elastic fracture mechanics asserts that

$$K_{1A}^2 \leq K_{1C}^2 \equiv \frac{2E\Gamma_o}{1 - \nu^2} \tag{116}$$

If the unknown equilibrium shape of the crack periphery, under both the influences of  $K_{1A}$  and  $\Sigma_o$ , has a tip radius  $R_t$ , then the *effective stress intensity factor*  $K_{1E}$  is

$$K_{IE} = K_{IA} + K_{I\Sigma}(R_t) = K_{IA} - \frac{2\Sigma_0}{\sqrt{\pi R_t}} \quad (117)$$

where (115) has been used. The effective stress-intensity factor is responsible for the tip radius. It follows from (111) that

$$R_t = \left[ \frac{2(1-\nu^2)}{\sqrt{\pi E}} \left( K_{IA} - \frac{2\Sigma_0}{\sqrt{\pi R_t}} \right) \right]^2 \quad (118)$$

which may be solved for  $R_t$ . The result is

$$\sqrt{R_t} = \frac{(1-\nu^2)K_{IA}}{\sqrt{\pi E}} \left\{ 1 + \left[ 1 - \frac{4\Sigma_0 E}{(1-\nu^2)K_{IA}^2} \right]^{1/2} \right\} \quad (119)$$

which is valid only for

$$K_{IA}^2 \geq \frac{4E\Sigma_0}{(1-\nu^2)} = 2cK_{IC}^2. \quad (120)$$

The origin of this condition follows from (115) that the reduction is inversely proportional to the tip radius. The effective stress-intensity factor is now given by

$$K_{IE} = K_{IA} \left\{ 1 - \frac{c(K_{IC}/K_{IA})^2}{1 + [1 - 2c(K_{IC}/K_{IA})^2]^{1/2}} \right\} \quad (121)$$

where  $c$  was defined in (74).

It is now convenient to introduce dimensionless stress intensity factors  $k_E$  and  $k_A$  as follows:

$$k_E = K_{IE}/K_{IC}, \quad k_A = K_{IA}/K_{IC}. \quad (122)$$

Substituting the above into (121), we get

$$k_E = [k_A^2 + k_A(k_A^2 - 2c)^{1/2} - c] / [k_A + (k_A^2 - 2c)^{1/2}], \quad (123)$$

which is an estimate for  $k_E$  in terms of  $k_A$ , and is valid only for  $k_A^2 > k_{AO}^2(c) = 2c$ . We have

$$k_E|_{k_A=k_{AO}} = k_{EO}(c) = \frac{1}{2}k_{AO}(c), \quad (124)$$

$$\partial k_E / \partial k_A = \infty \quad \text{for} \quad k_A = k_{AO}(c). \quad (125)$$

It is clear from (123)–(125) and Fig. 5 that

$$k_E \geq k_{EO}(c), \quad k_E/k_A = K_{IE}/K_{IA} \leq 1 \quad \text{for} \quad k_A \geq k_{AO}(c) \quad (126)$$

for all  $c$ . Since the modified fracture criterion is

$$k_E = K_{IE}/K_{IC} \leq 1, \quad (127)$$

we conclude from the first of (126) that

$$k_{EO}(c) \leq 1 \quad \text{or} \quad c = \Sigma_o/\Gamma_o \leq 2. \quad (128)$$

Setting  $k_E = 1$  in (123), we find

$$k_A = k_{AC}(c) = 1 + c/2 \quad \text{for} \quad 0 \leq c \leq 2, \quad (129)$$

which shows the toughness enhancement:

$$K_{IA} < (1 + c/2)K_{IC} \quad \text{for} \quad 0 \leq c \leq 2. \quad (130)$$

The maximum possible enhancement is a doubling in  $K_{IC}$  when  $\Sigma_o$  is exactly  $2\Gamma_o$ .

Chuang (1987) showed in a calculation that the toughness could be enhanced by as much as three times the intrinsic  $K_{IC}$  value. His analysis began with the surface energy density  $\gamma$ , measured per unit surface area in the deformed configuration. In terms of our notation,

$$\gamma = \Gamma/\Lambda = \Gamma_o + (\Sigma_o - \Gamma_o)\varepsilon, \quad (131)$$

and his surface stress  $\tau$  is

$$\tau = \Gamma_o + \partial\gamma/\partial\varepsilon = \Sigma_o. \quad (132)$$

In his calculation,  $\partial\gamma/\partial\varepsilon = \Sigma_o - \Gamma_o$  was taken to be  $3\Gamma_o$  so that  $\tau = \Sigma_o = 4\Gamma_o$ . If we blindly let  $c = 4$  in (130), the enhancement factor turns out to be exactly 3, but our approximation is valid only for  $c \leq 2$ . Nevertheless, the two approximate results appear to be in good qualitative agreement.

## 5. Summary

The configurational equilibrium of a void in a stressed body, under the action of traction  $T$ , may be altered by the presence of a surface stress  $\Sigma_o$  via the interaction energy formed by  $\Sigma_o$  and  $T$ . For geometrically smooth voids the affected changes are small, but sensitive to the sign of  $T$ . Geometric singularities such as notch- and crack-tips are the sites where severe deformations occur. The presence of surface stress has the capability of containing the severity of these deformations.

## References

- Asaro, R.J., Tiller, W.A., 1972. Interface morphology development during stress corrosion cracking: Part I. Via surface diffusion. *Met. Trans.* 3, 1789–1796.
- Chiu, C.H., Gao, H., 1993. Stress singularities along a cycloid rough surface. *Int. J. Solids Structures* 30, 1983–3012.

- Chuang, T.-J., 1987. Effect of surface tension on the toughness of glass. *J. Am. Ceram. Soc.* 70, 160–164.
- Ferrante, J., Smith, J.R., Rose, J.H., 1983. Diatomic molecules and metallic adhesion, cohesion, and chemisorption: a single binding-energy relation. *Physical Review Letters* 50, 1385–1386.
- Freund, L.B., 1995. Evolution of waviness on the surface of a strained elastic solid due to stress-driven diffusion. *Int. J. Solids Structures* 32, 911–923.
- Freund, L.B., 1998. A surface chemical potential for elastic solids. *J. Mech. Phys. Solids* 46, 1835–1844.
- Gao, H., 1991. A boundary perturbation analysis for elastic inclusions and interfaces. *Int. J. Solids Structures* 28, 703–725.
- Gao, H., 1995. Mass-conserved morphological evolution of hypocycloid cavities: a model of diffusive crack initiation with no associated energy barrier. *Proc. R. Soc. Lond. A* 488, 465–483.
- Grilhe, J., 1993. Study of roughness formation induced by homogeneous stress at the free surfaces of solids. *Acta Metall. Mater.* 41, 909–913.
- Grinfeld, M.A., 1986. Instability of the separation boundary between a nonhydrostatically stressed elastic body and a melt. *Sov. Phys. Dokl.* 31, 831–834.
- Grinfeld, M.A., 1994. Stress corrosion and stress induced surface morphology of epitaxial films. *Scanning Microscopy* 8, 869–882.
- Gurtin, M.E., Murdoch, A.I., 1978. Surface stress in solids. *Int. J. Solids Structures* 14, 431–440.
- Leo, P.H., Sekerka, R.F., 1989. The effect of surface stress on crystal-melt and crystal-crystal equilibrium. *Acta Metall.* 37, 3119–3138.
- Murr, L.E., 1975. *Interfacial Phenomena in Metals and Alloys*. Addison-Wesley.
- Norris, A.N., 1998. The energy of a growing elastic surface. *Int. J. Solids Structures* 35, 5237–5252.
- Rice, J.R., Chuang, T.J., 1981. Energy variations in diffusive cavity growth. *J. Amer. Ceramic Soc.* 64, 46–53.
- Rose, J.H., Ferrante, J., Smith, J.R., 1981. Universal binding energy curves for metals and bimetallic interfaces. *Physical Review Letters* 47, 675–678.
- Rose, J.H., Smith, J.R., Ferrante, J., 1983. Universal features of bonding in metals. *Physical Review B* 28, 1835–1845.
- Suo, Z., Wang, W., 1994. Diffusive void bifurcation in stressed solid. *J. Appl. Phys.* 76, 3410–3421.
- Spencer, B.J., Meiron, D.I., 1994. Nonlinear evolution of the stress-driven morphological instability in a two dimensional semi-infinite solid. *Acta Metall. Mater.* 42, 3629–3641.
- Srolovitz, D., 1989. On the stability of surfaces of stressed solids. *Acta Metall.* 37, 621–625.
- Wang, W., Suo, Z., 1997. Shape change of a pore in a stressed solid via surface diffusion motivated by surface and elastic energy variation. *J. Mech. Phys. Solids* 45, 709–729.
- Wu, C.H., 1979. Plane-strain buckling of a crack in a harmonic solid subjected to crack-parallel compression. *J. Appl. Mech.* 46, 597–603.
- Wu, C.H., 1980. Plane-strain buckling of cracks in incompressible solids. *J. Elasticity* 10, 163–177.
- Wu, C.H., 1996. The chemical potential for stress-driven surface diffusion. *J. Mech. Phys. Solids* 44, 2059–2077.
- Wu, C.H., Hsu, J.H., Chen, C.H., 1998. The effect of surface stress on the stability of surfaces of stressed solids. *Acta Materialia* 46, 3755–3760.
- Yang, W.H., Srolovitz, D.J., 1994. Surface morphology evolution in stressed solids: surface diffusion controlled crack initiation. *J. Mech. Phys. Solids* 42, 1551–1574.